Journal of Magnetic Resonance **140,** 108–119 (1999)
Article ID jmre.1999.1833, available online at http://www.idealibrary.com on IDEAL®

Spectral Fitting of NMR Spectra Using an Alternating Optimization Method with *a Priori* Knowledge[1]

Zhaoqiang Bi,* Angela P. Bruner,† Jian Li,*,[2] Katherine N. Scott,‡ Zheng-She Liu,§,[3]
Christine B. Stopka,¶ Hee-Won Kim,‖ and David C. Wilson**

**Department of Electrical and Computer Engineering, P.O. Box 116130, University of Florida, Gainesville, Florida 32611; †Department of Radiology, P.O. Box 100374, University of Florida, Gainesville, Florida 32611; ‡Department of Radiology, Physics, and Nuclear Radiological Sciences, P.O. Box 100374, University of Florida, and the Veteran Affairs Medical Center, Gainesville, Florida 32610; §Department of Electrical and Computer Engineering, P.O. Box 116130, University of Florida, Gainesville, Florida 32611; ¶Department of Exercise and Sports Sciences, P.O. Box 118205, University of Florida, Gainesville, Florida 32611; ‖Department of Radiology and Neuroscience, P.O. Box 100374, University of Florida, Gainesville, Florida 32610; and **Department of Mathematics, P.O. Box 118105, University of Florida, Gainesville, Florida 32611*

Received October 16, 1998; revised May 27, 1999

As alternatives to the fast Fourier transform, advanced parametric methods based on the damped sinusoidal data model have been devised to better quantify the nuclear magnetic resonance (NMR) spectroscopy time-domain data. Previously, linear prediction (LP) fitting methods using Householder triangularization and singular value decomposition (SVD) techniques have been applied to the NMR spectroscopy data analysis. In this paper, we propose an alternating optimization method to quantify the time-domain NMR spectroscopy data. The proposed algorithm uses the *a priori* knowledge of the possible frequency intervals of the damped sinusoids to obtain more accurate parameter estimates when the NMR spectroscopy data are obtained under low signal-to-noise ratio conditions and the peaks are close together. None of the LP and SVD type of methods can use such approximate *a priori* knowledge. We have shown with measured NMR spectroscopy data that the proposed algorithm can be used to obtain accurate parameter estimates of frequencies, amplitudes, and damping ratios of the damped sinusoids and therefore the ultimate fit of the spectrum by using the *a priori* knowledge about the possible frequency intervals of the damped sinusoids.

1. INTRODUCTION

Fast Fourier transform (FFT) is widely used in the spectral analysis of nuclear magnetic resonance (NMR) spectroscopy time-domain signals due to its computational efficiency. FFT is usually performed on the time-domain free induction decay (FID) in conjunction with zero-filling and appropriate apodization (usually Gaussian or exponential multiplication or line broadening) of the time-domain FIDs to obtain high spectral sampling resolution and signal-to-noise ratio (SNR) within the frequency-domain spectra (*1*). However, the frequency resolution achieved by the FFT method is poor when the FIDs are strongly damped or truncated and the apodization process can result in spectral leakage. This ultimately creates reduced areas in some or all of the postprocessed spectrum peaks. These drawbacks become even worse when the spectral frequencies are closely spaced and the FID data are recorded under low SNR conditions.

Since the NMR spectroscopy time-domain data can be represented as the sum of several damped sinusoids characterized by the frequencies of the measured metabolites and their associated peak amplitudes and damping ratios (due to relaxation effects dominated by T_2^*), advanced parametric spectral estimation algorithms can be used as alternatives for analyzing the time-domain NMR spectroscopy data. Maximum entropy methods (MEM) (*2–5*) and linear prediction (LP) methods using Householder triangularization (*6*) and singular value decomposition (SVD) (*7–10*) techniques have shown considerable promise in providing reliable parameter estimates for the NMR spectroscopy data. The location estimates of the spectral peaks obtained by LP-based methods can be greatly affected by a small amount of noise (*7*) and their accuracy can be improved by singular value decomposition of the LP data matrix. At low SNR, the total least-squares (TLS) techniques (*11*, *12*) can be used to further improve the accuracy of LP- and SVD-based methods. Recently, maximum likelihood (ML) methods (*13–15*) have been used to provide frequency estimates with superior resolution for NMR spectroscopy data analysis. A robust alternating optimization method, referred to as RELAX (*16*), has also been proposed to estimate the damped sinusoidal signal parameters.

All these methods, however, do not apply any *a priori* knowledge of the signal parameters except for the assumed

[1] This work was supported in part by the National Science Foundation under Grant MIP-9457388 and the Veterans Affairs Medical Research Service.

[2] To whom correspondence should be addressed. Fax: (352) 392-0044. E-mail: li@dsp.ufl.edu.

[3] Present address: OEM Research & Development, 3COM Corp., 7770 N. Frotage Road, Skokie, IL 60076-2690.

1090-7807/99 $30.00

damped sinusoidal data model. Some *a priori* knowledge about the signal parameters, such as the rigorous knowledge of the exactly known frequency locations and damping ratios or the more flexible knowledge of the possible frequency intervals of the damped sinusoids, may be available to further improve the resolution and accuracy of the parameter estimates. In (*17, 18*), the knowledge of the *exactly known signal poles* has been used to improve the parameter estimates. The variable projection method (VARPRO) has been used in (*19*) for accurate quantification of *in vivo* ^{31}P NMR signals by utilizing the *a priori* knowledge of the model function and the phases of all spectral components.

In this paper, we extend the RELAX algorithm (*16*) to the case when the more flexible *a priori* knowledge of the possible *frequency intervals* of the peak locations, rather than that of the *exact locations of the peaks* or the *exact values of the damping ratios*, is available. The extended RELAX algorithm is referred to as the E-RELAX algorithm. We have demonstrated with numerical examples the performances of RELAX and the fast ML (FML) method (*14*) for signal parameter estimation. RELAX outperforms FML when the SNR is low. When the SNR is high, RELAX and FML achieve almost identical performance. We also modify FML by utilizing the *a priori* knowledge of frequency intervals and the so-obtained method is referred to as E-FML. Both E-RELAX and E-FML have been applied to low SNR phosphorus (^{31}P) spectroscopy datasets, whose spectra have overlapping peaks, rapidly changing peak heights, and spectral frequency changes. The experimental results show that both methods provide consistent frequency estimates by incorporating the *a priori* knowledge of the possible frequency intervals of the damped sinusoids for the low SNR ^{31}P spectroscopy data. The spectroscopy analysis based on the parameter estimates of E-RELAX more accurately reflects the metabolic change of the subject than that based on those of E-FML for the metabolite peak P_i.

The remainder of this paper is organized as follows. Section 2 briefly describes the E-RELAX algorithm for the damped sinusoidal signal parameter estimation by using the *a priori* knowledge of the possible frequency intervals. Section 3 presents both numerical and experimental examples showing the performances of E-RELAX and E-FML when compared with the original RELAX algorithm, the best SVD method (*10*), and FML (*14*) without using any of the *a priori* knowledge of the possible frequency intervals of the damped sinusoids. Finally, Section 4 contains our conclusions.

2. ALGORITHMS

The time-domain NMR spectroscopy data can be represented as the sum of several damped complex sinusoids, each of which has its own characteristic frequency, damping ratio, amplitude, and phase. Let $y(n)$ denote a time-domain NMR spectroscopy data sequence consisting of K exponentially decaying sinusoids in the presence of unknown noise. Then

$$y(n) = \sum_{k=1}^{K} \alpha_k e^{(-d_k + j\omega_k)n} + e(n), \quad n = 0, 1, \ldots, N-1, \tag{1}$$

where α_k and ω_k, respectively, denote the complex amplitude and frequency of the kth damped sinusoid whose damping ratio is d_k with $d_k \in \mathcal{R}^+$; $e(n)$ is the unknown additive noise.

The problem of interest herein is to estimate the parameters $\{d_k, \omega_k, \alpha_k\}_{k=1}^{K}$ from the data sequence $\{y(n)\}_{n=0}^{N-1}$ by utilizing the available *a priori* knowledge of the possible frequency intervals of the damped sinusoids. The quantification of the NMR spectroscopy data can then be easily accomplished based on the parameter estimates.

2.1. The RELAX Algorithm

The RELAX algorithm (*16*) has been proposed to estimate the damped sinusoidal signal parameters based on the data model in [1] without considering any *a priori* knowledge of the signal parameters. RELAX obtains the parameter estimates $\{\hat{d}_k, \hat{\omega}_k, \hat{\alpha}_k\}_{k=1}^{K}$ of $\{d_k, \omega_k, \alpha_k\}_{k=1}^{K}$ by minimizing the following NLS criterion,

$$C(\{d_k, \omega_k, \alpha_k\}_{k=1}^{K}) = \Big\|\mathbf{y} - \sum_{k=1}^{K} \alpha_k \boldsymbol{\phi}_k\Big\|^2, \tag{2}$$

where $\|\cdot\|$ denotes the Euclidean norm (*20*),

$$\mathbf{y} = [y(0)\ y(1)\ \cdots\ y(N-1)]^{\mathrm{T}}, \tag{3}$$

and

$$\boldsymbol{\phi}_k = [1\ e^{(-d_k + j\omega_k)}\ \cdots\ e^{(-d_k + j\omega_k)(N-1)}]^{\mathrm{T}}, \tag{4}$$

with $(\cdot)^{\mathrm{T}}$ denoting the transpose. RELAX utilizes the same structure as in (*21*) to optimize the NLS cost function. Note that when the noise $e(n)$ is a zero-mean white Gaussian random process, the NLS estimates coincide with the ML estimates. When the noise is colored, the NLS estimates are no longer the ML estimates, but they can still have excellent statistical performance (*22*).

To efficiently optimize the complicated NLS cost function in [2], RELAX performs a complete alternating search by letting only the parameters of one damped sinusoid vary and fixing all others at their most recently determined values. Let $\bar{K}$ denote the intermediate number of damped sinusoids and given $\{\hat{\alpha}_i, \hat{d}_i, \hat{\omega}_i\}_{i=1, i\neq k}^{\bar{K}}$. Then the estimates of $\{d_k, \omega_k\}$ can be determined by

$$\{\hat{d}_k,\ \hat{\omega}_k\} = \arg\max_{d_k,\omega_k}\{|\boldsymbol{\psi}_k^{\mathrm{H}}\tilde{\mathbf{y}}_k|^2/a\}, \quad [5]$$

where $(\cdot)^{\mathrm{H}}$ denotes the complex conjugate transpose;

$$a = \begin{cases} N, & \text{if } d_k = 0, \\ \dfrac{1-\exp(-2Nd_k)}{1-\exp(-2d_k)}, & \text{if } d_k \neq 0; \end{cases} \quad [6]$$

$$\mathbf{y}_k = \mathbf{y} - \sum_{i=1, i\neq k}^{\bar{K}} \hat{\alpha}_i \hat{\boldsymbol{\phi}}_i, \quad [7]$$

with $\hat{\boldsymbol{\phi}}_i$ having the same form as $\boldsymbol{\phi}_k$ in [4] except that d_i and ω_i are replaced by $\hat{d}_i$ and $\hat{\omega}_i$, respectively;

$$\tilde{\mathbf{y}}_k = [y_k(0)\ y_k(1)e^{-d_k}\cdots y_k(N-1)e^{-d_k(N-1)}]^{\mathrm{T}}; \quad [8]$$

and finally

$$\boldsymbol{\psi}_k = [1\ e^{j\omega_k}\cdots e^{j\omega_k(N-1)}]. \quad [9]$$

The estimate of α_k can be determined by

$$\hat{\alpha}_k = \left.\frac{\sum_{n=0}^{N-1} y_k(n)e^{(-d_k+j\omega_k)n}}{a}\right|_{d_k=\hat{d}_k,\omega_k=\hat{\omega}_k}. \quad [10]$$

It has been shown in (*16*) that for a fixed d_k, the $\hat{\omega}_k(d_k)$ can be obtained as the location of the dominant peak of the normalized periodogram $|\boldsymbol{\psi}_k^{\mathrm{H}}\tilde{\mathbf{y}}_k(d_k)|^2/a(d_k)$, which can be computed efficiently via FFT with zero-filling ($\hat{\omega}_k(d_k)$, $\tilde{\mathbf{y}}_k(d_k)$, and $a(d_k)$ indicate the dependence of $\hat{\omega}_k$, $\tilde{\mathbf{y}}_k$, and a on d_k). Then the problem of solving [5] becomes finding $\hat{d}_k$ such that the right side of [5] is maximized, i.e.,

$$\hat{d}_k = \arg\max_{d_k}\left\{\frac{|\boldsymbol{\psi}_k^{\mathrm{H}}[\hat{\omega}_k(d_k)]\tilde{\mathbf{y}}_k(d_k)|^2}{a(d_k)}\right\}, \quad [11]$$

which can be implemented by a typical 1D search. The search interval for $\{d_k\}_{k=1}^K$ used in our examples in Section 3 is from 0.0015 to 0.05. Once $\hat{\omega}_k$ and $\hat{d}_k$ are obtained, $\hat{\alpha}_k$ can be readily obtained via [10].

Then the steps of the RELAX algorithm are summarized as follows.

Step 1. Assume $\bar{K} = 1$. Estimate $\{\hat{d}_1,\ \hat{\omega}_1,\ \hat{\alpha}_1\}$ from $\mathbf{y}$.

Step 2. Assume $\bar{K} = 2$. Compute $\mathbf{y}_2$ with [7] by using $\{\hat{d}_1,\ \hat{\omega}_1,\ \hat{\alpha}_1\}$ obtained in Step 1. Obtain $\{\hat{d}_2,\ \hat{\omega}_2,\ \hat{\alpha}_2\}$ from $\mathbf{y}_2$. Next, compute $\mathbf{y}_1$ with [7] by using $\{\hat{d}_2,\ \hat{\omega}_2,\ \hat{\alpha}_2\}$ and then reestimate $\{\hat{d}_1,\ \hat{\omega}_1,\ \hat{\alpha}_1\}$ from $\mathbf{y}_1$.

Iterate the previous two substeps until "practical convergence" is achieved (to be discussed later on).

Step 3. Assume $\bar{K} = 3$. Compute $\mathbf{y}_3$ with [7] by using $\{\hat{d}_i,\ \hat{\omega}_i,\ \hat{\alpha}_i\}_{i=1}^2$ obtained in Step 2. Obtain $\{\hat{d}_3,\ \hat{\omega}_3,\ \hat{\alpha}_3\}$ from $\mathbf{y}_3$. Next, compute $\mathbf{y}_1$ with [7] by using $\{\hat{d}_i,\ \hat{\omega}_i,\ \hat{\alpha}_i\}_{i=2}^3$ and redetermine $\{\hat{d}_1,\ \hat{\omega}_1,\ \hat{\alpha}_1\}$ from $\mathbf{y}_1$. Then compute $\mathbf{y}_2$ with [7] by using $\{\hat{d}_i,\ \hat{\omega}_i,\ \hat{\alpha}_i\}_{i=1,3}$ and redetermine $\{\hat{d}_2,\ \hat{\omega}_2,\ \hat{\alpha}_2\}$ j from $\mathbf{y}_2$.

Iterate the previous three substeps until practical convergence.

Remaining steps. Continue similarly until $\bar{K}$ is equal to the desired or estimated number of damped sinusoids. Note that for each $\bar{K}$, the iteration of the $\bar{K}$ substeps continues until practical convergence is achieved.

The practical convergence in the iterations of the above RELAX algorithm may be determined by checking the relative change of the cost function $C(\{\hat{d}_i,\ \hat{\omega}_i,\ \hat{\alpha}_i\}_{i=1}^K)$ in [2] between two consecutive iterations. In our examples, we terminate the iterative process in each of the above steps when the aforementioned relative change is less than $\xi = 10^{-3}$. Although not guaranteed to converge to the global minimum, it has been shown with many numerical and empirical examples used in many papers that the alternating optimization method is very useful and converges to at least a local minimum under mild condition. The convergence issue of the alternating optimization method is addressed in (*23*, *24*).

2.2. The E-RELAX Algorithm

In NMR spectroscopy, the possible intervals of some or all of the frequencies of the damped sinusoids may be known *a priori*. We attempt to obtain more accurate estimates of $\{d_k,\ \omega_k,\ \alpha_k\}_{k=1}^K$ by incorporating this type of *a priori* knowledge into the RELAX algorithm. This extended algorithm is referred to as E-RELAX. The principal difference between RELAX and E-RELAX lies in the maximization of [5]. Let $\boldsymbol{\zeta}_k$ be a possible frequency interval, during which there exists only one dominant damped sinusoid with frequency ω_k. Then the estimates of $\{d_k,\ \omega_k\}$ are now determined by

$$\{\hat{d}_k,\ \hat{\omega}_k\} = \arg\max_{d_k,\omega_k\in\boldsymbol{\zeta}_k}\{|\boldsymbol{\psi}_k^{\mathrm{H}}\tilde{\mathbf{y}}_k|^2/a\}. \quad [12]$$

Equation [12] indicates that the 1D search for ω_k is now limited to the interval $\boldsymbol{\zeta}_k$ rather than the entire possible range. Let $\{\boldsymbol{\zeta}_{oi}\}_{i=1}^K$ denote the given *a priori* frequency intervals of the damped sinusoids. $\{\hat{\omega}_i\}_{i=1,i\neq k}^{\bar{K}}$ is given. Then

$$\boldsymbol{\zeta}_k = \bigcup_{i=1}^{K}(\boldsymbol{\zeta}_{oi}) - \bigcup_{i=1,i\neq k}^{\bar{K}}(\boldsymbol{\beta}_i), \quad [13]$$

where $\cup$ denotes the union of sets and the $\bar{K}-1$ frequency intervals $\{\boldsymbol{\beta}_i\}_{i=1,i\neq k}^{\bar{K}}$ are determined by checking $\{\hat{\omega}_i\}_{i=1,i\neq k}^{\bar{K}}$ with the given *a priori* frequency intervals. The steps of

E-RELAX are similar to those of RELAX except for the extra constraints imposed by ζ_k for E-RELAX. Note that when the baseline distortion is severe, E-RELAX can still be used to fit the NMR spectroscopy data after the correction of the baseline distortion with the existing baseline distortion correction methods, such as those in (*25*).

2.3. FML Methods

The FML method (*14*) was proposed for the damped sinusoid parameter estimation in a fast manner. FML belongs to an alternating optimization approach and reduces the computation complexity of the ML methods by utilizing the knowledge of the shape of the compressed likelihood function. The statistical performance and computational efficiency of FML have been demonstrated in (*14*) when compared with other methods based on alternating projections and linear prediction. See (*14*) for the detailed implementation steps of FML.

We modify FML by using the *a priori* knowledge of the frequency intervals of the metabolite peaks. The so-obtained method is referred to as E-FML. E-FML obtains the frequency estimate of each damped sinusoid by searching a possible frequency interval, which is determined in the same way as that of E-RELAX.

2.4. The Analysis of the NMR Spectroscopy Data

With the accurate estimates of $\{d_k,\ \omega_k,\ \alpha_k\}_{k=1}^{K}$, we can analyze and fit the spectrum of the NMR spectroscopy data, including the analysis of the phased absorption spectrum and the calculation of the relative areas corresponding to the metabolite peaks of interest.

The positive and symmetric absorption spectrum is commonly used for NMR spectroscopy data analysis. Theoretically, the absorption is confined to the real part of the Lorentzian spectrum with the phases of the damped sinusoids being zero (*1*). In practice, the phases of the damped sinusoids cannot be zeros due to a variety of reasons, such as the phase difference between the transmitter and detector of the spectrometer and a delay in the start of the free induction decay collection. The introduced phases will distort the absorption spectrum and must be corrected to obtain a pure absorption spectrum. As indicated in (*6, 26*), as long as the phases and other parameters of the damped sinusoids can be estimated correctly, the phase absorption spectrum corresponds to the real part of the phased Lorentzian spectrum obtained by setting the phases of all the decay sinusoids to zero. Specifically, the phased spectrum of the measured FIDs can be obtained by applying FFT to the synthesized damped sinusoidal data sequence $\{y_s(n)\}_{n=0}^{N_s-1}$ with the phases of all damped sinusoids set to zero, where N_s denotes the number of the synthesized data samples and

$$y_s(n) = \sum_{k=1}^{K} |\hat{\alpha}_k| e^{(-\hat{d}_k + j\hat{\omega}_k)n}, \quad n = 0, 1, \ldots, N_s - 1. \tag{14}$$

We choose N_s to be sufficiently large so that $y_s(N_s - 1) \approx 0$. Then the phased absorption spectrum can be obtained by taking the real part of the so-obtained phased spectrum. We use a simulation example to illustrate this phase correction method. The data sequence is generated by using

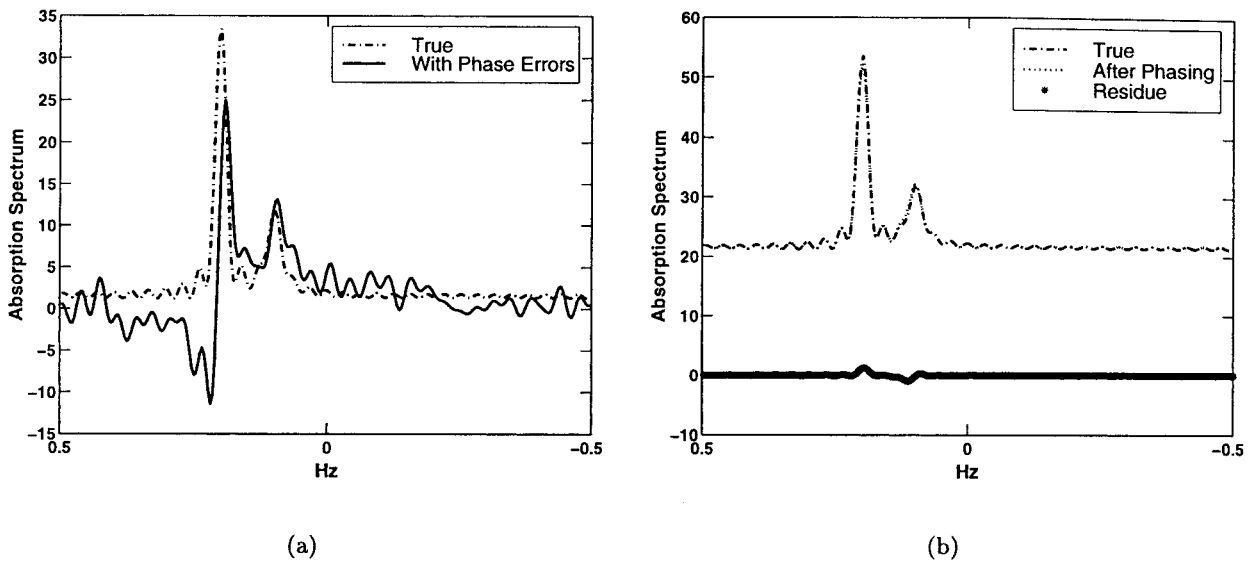

FIG. 1. Illustration of the proposed phase correction method in the presence of zero-mean complex Gaussian noise with $\sigma^2 = 0.1$. (a) The true absorption spectrum (· - · -) and the distorted absorption spectrum (—). (b) Comparison of the phased absorption spectrum and the true absorption spectrum.

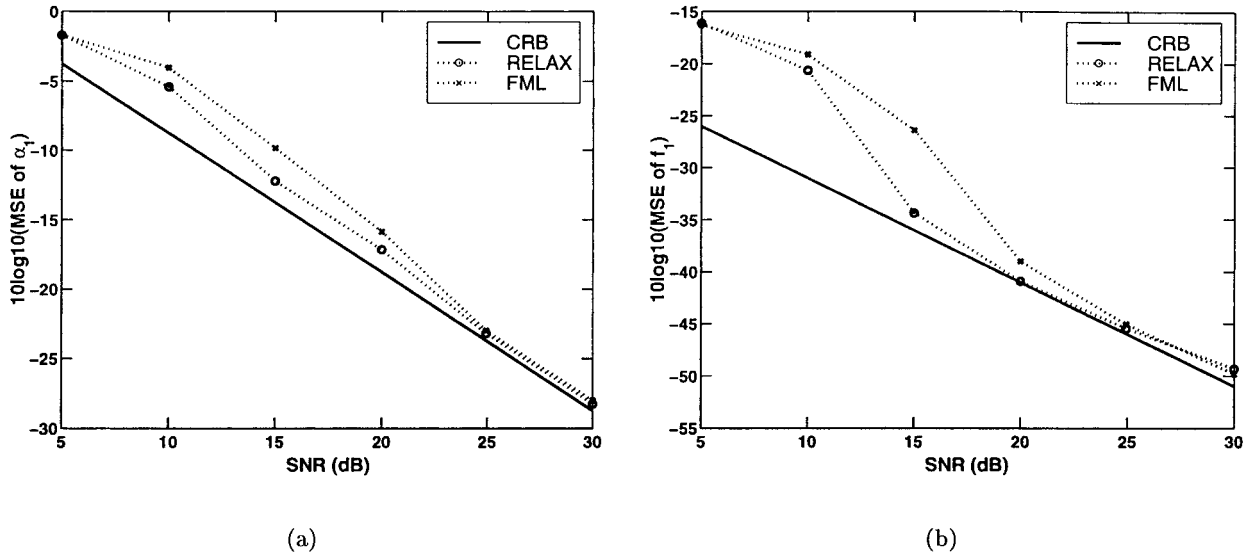

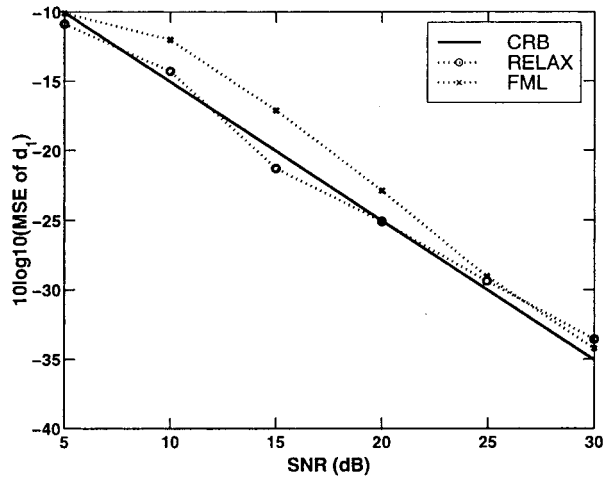

(c)

FIG. 2. CRBs (solid line) and MSEs of the damped sinusoidal parameter estimates of the first of the $K = 2$ signals obtained via RELAX and FML as a function of SNR in the presence of white noise when $N = 25$. (a) For $\alpha_1 = 1$. (b) For $f_1 = 0.42$. (c) For $d_1 = 0.4$.

$$y(n) = e^{j\phi_1}e^{[-0.1+j2\pi(0.1)]n} + e^{j\phi_2}e^{[-0.05+j2\pi(0.2)]n} + e(n), \quad n = 0, 1, \ldots, N-1, \quad [15]$$

where $N = 25$; ϕ_1 and ϕ_2, respectively, denote the phases of the two damped sinusoids; and $e(n)$ is the zero-mean white complex Gaussian noise with $\sigma^2 = 0.1$. Figure 1a shows the true absorption spectrum (denoted by the dash-dotted line) with $\phi_1 = \phi_2 = 0$. The distorted absorption spectrum obtained with $\phi_1 = \pi/6$ and $\phi_2 = \pi/3$ is also shown in Fig. 1a (denoted by the solid line). The phased absorption spectrum based on the parameter estimates via RELAX is shown in Fig. 1b (denoted by the dotted line). The residue between the phased spectrum and the true one, as shown in Fig. 1b, demonstrates that the so-obtained phased absorption spectrum fits very well to the true absorption spectrum.

The relative area for a defined region of the spectrum spanning the metabolite peak of interest provides a quantitative estimate of the concentration of spins giving rise to the NMR spectroscopy data. With $\hat{\alpha}_k$ and $\hat{d}_k$, the absorption spectrum corresponding to the kth metabolite peak has the form

$$P_k(\omega) = \frac{|\hat{\alpha}_k|\hat{d}_k}{\hat{d}_k^2 + \omega^2}, \quad [16]$$

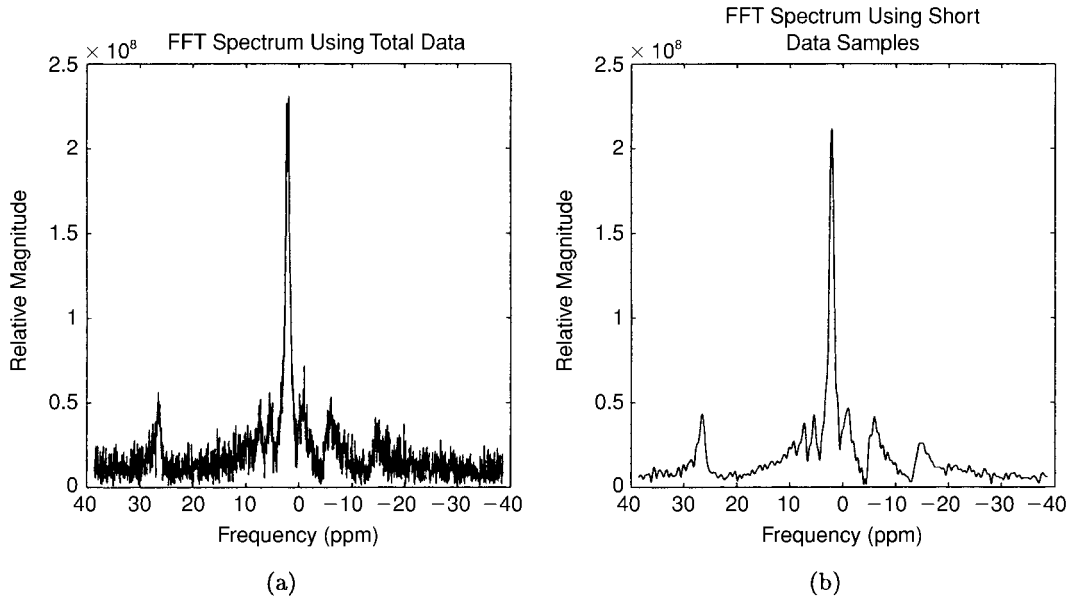

FIG. 3. (a) The FFT spectrum obtained from the total NMR spectroscopy data. (b) The FFT spectrum obtained by using the first 100 points of the original data.

which is the real part of the Fourier transform of the kth estimated damped sinusoid whose phase is set to zero. According to Parseval's theorem (*27*), we have

$$E_k = \sum_{n=0}^{N_s-1} (|\hat{\alpha}_k| e^{-\hat{d}_k n})^2 = \frac{1}{2\pi} \int_{-\pi}^{\pi} \frac{|\hat{\alpha}_k|^2}{\hat{d}_k^2 + \omega^2} d\omega. \quad [17]$$

The area of $P_k(\omega)$ can then be easily computed as

$$S_k = \int_{-\pi}^{\pi} \frac{|\hat{\alpha}_k| \hat{d}_k}{\hat{d}_k^2 + \omega^2} d\omega = \frac{2\pi E_k \hat{d}_k}{|\hat{\alpha}_k|}, \quad k = 1, 2, \ldots, K, \quad [18]$$

where E_k is computed by using the first equality in [17].

3. NUMERICAL AND EXPERIMENTAL RESULTS

In this section, we first compare the performances of RELAX and FML with a numerical example and then compare RELAX and the best SVD method (*10*) using the measured NMR spectroscopy data since it has been shown in (*16*) that RELAX outperforms the SVD method in performance with numerical examples. Finally, the performances of E-RELAX and E-FML are compared with the measured NMR spectroscopy datasets.

Consider first a numerical example showing the performances of RELAX and FML for the signal parameter estimation when compared with the Cramér–Rao bound (CRB), which is the lowest bound that an unbiased estimator can achieve. The mean-squared errors (MSEs) of the parameter estimates are determined from 500 independent Monte Carlo trials. In this example, the data sequence is generated by using

$$y(n) = e^{s_1 n} + e^{s_2 n} + e(n), \quad n = 0, 1, \ldots, N-1, \quad [19]$$

where $N = 25$, $s_1 = -0.4 + j2\pi(0.42)$, $s_2 = -0.07 + j2\pi(0.52)$, and $e(n)$, as before, is the zero-mean white complex Gaussian noise with variance σ^2. The SNR herein is defined as $-10 \log_{10}(\sigma^2)$ dB. Figures 2a–2c show the MSEs of the estimates of α_1, f_1, and d_1, as a function of SNR via RELAX and FML. (Note that the results for α_2, f_2, and d_2 are similar.) The MSEs of the parameter estimates obtained via both methods approach the corresponding CRBs for high SNR. However, RELAX provides better performance than FML for low SNR. We also note that at low SNR, RELAX and FML are comparable in computation. However, the average number of MATLAB flops required by FML is about 1.7 times of that required by RELAX at high SNR.

Consider next an example where the measured time-domain NMR spectroscopy data sequence consists of 2048 samples. Specifically, these data samples are 64 acquisition-averaged phosphorus NMR spectra obtained from the medial gastrocnemius muscle at 1.5 T (GE Signa) (TR = 2 s, unlocalized, 6-cm-diameter ^{31}P-tuned coil). The spectrum of the data sequence has eight metabolite peaks representing, from left to right, STD (an external standard of hexachlorocyclotriphosphazene (HCCTP) and chromium acetate (CrOAc) in ben-

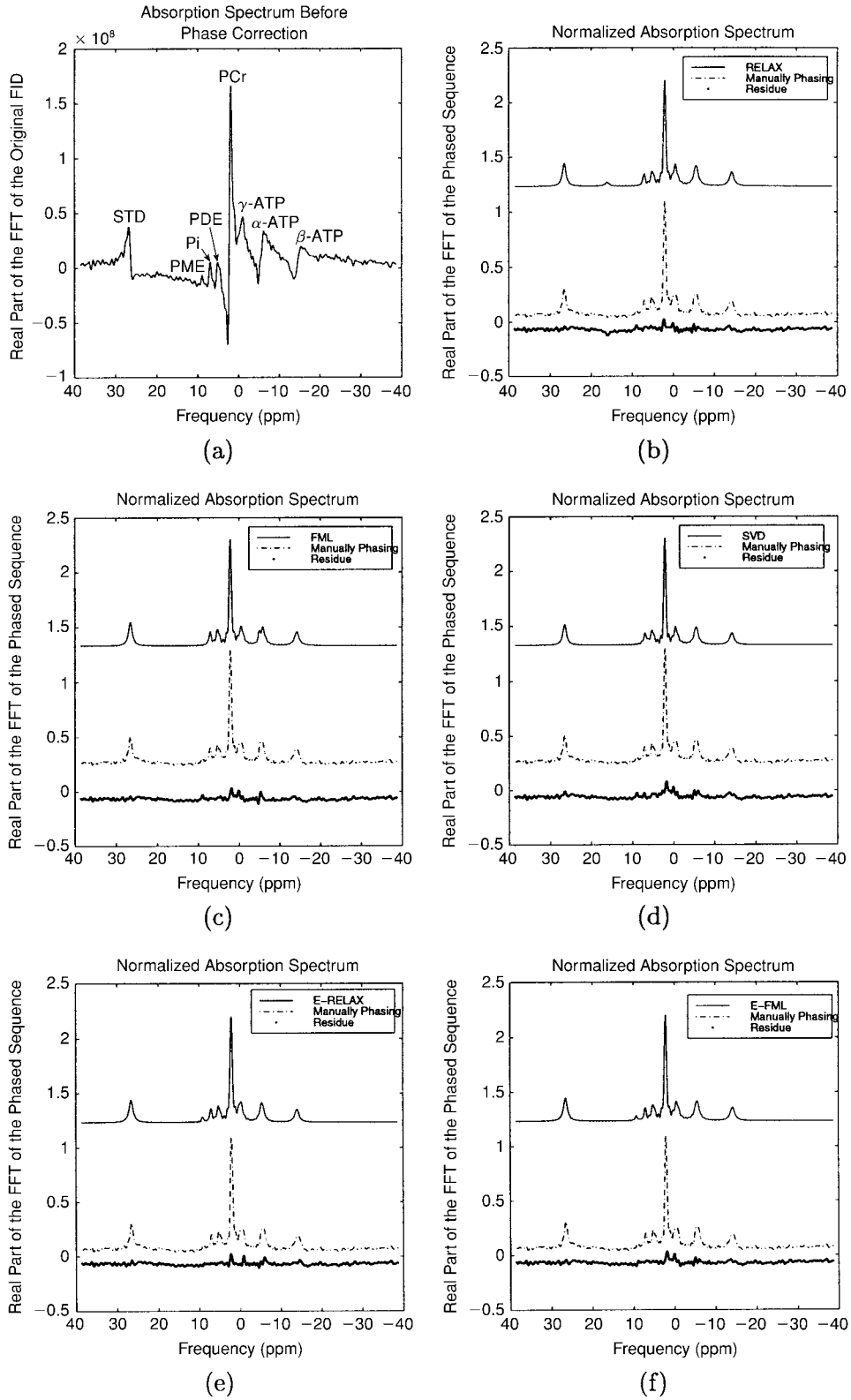

FIG. 4. Comparison of the manually phased absorption spectrum with the phased absorption spectra obtained via (b) RELAX, (c) FML, (d) SVD, (e) E-RELAX, and (f) E-FML. Note that the absorption before phase correction is shown in (a).

TABLE 1
The Approximate Frequency Locations of the Eight ^{31}P Metabolite Peaks of the Data Used in the First Experimental Example

	Peak							
	STD	PME	P_i	PDE	PCr	γ-ATP	α-ATP	β-ATP
Frequency (ppm)	26.57	9.06	7.11	5.29	2.11	−0.05	−5.29	−13.85

zene), PME (phosphomonoester), P_i (inorganic phosphate), PDE (phosphodiester), PCr (phosphocreatine), and γ-, α-, and β-ATP (adenosine triphosphate). Figures 3a and 3b, respectively, show the FFT spectrum obtained by using all the 2048 data samples and the first 100 data samples obtained by squarely truncating the original dataset without using any apodization. It is easier to distinguish the eight peaks in Fig. 3b than it is in Fig. 3a, which is dominated by noise. The absorption spectrum using the first 100 measured FIDs is shown in Fig. 4a, which indicates that phase correction is necessary to obtain a pure absorption spectrum. Only the peaks of labeled STD, P_i, and PCr arise from single compounds. The PME peak is generated by two metabolites: phosphatidylcholine (PC) and phosphatidylethanolamine (PE). The PDE peak is composed of glycerophosphorylcholine (GPC) and glycerophosphorylethanolamine (GPE). The peaks labeled α-, β-, and γ-ATP arise from nucleotide di- and triphosphates (NDP and NTP), mainly adenosine triphosphate (ATP). This is the reason that these peaks have been labeled "ATP." However, under *in vivo* conditions the spectroscopist is actually monitoring a summation of all the nucleotide di- and triphosphates present and not simply ATP. Therefore, the assignment of a resonance as "ATP" is not strictly accurate (*28*). In addition, only the β peak is a pure NTP (mainly ATP) signal. The γ peak contains contributions from both NTPs and NDPs. The α peak consists of NDPs, NTPs, and nicotinamide dinucleotide (NAD/NADH) (*29, 30*). Therefore, the three ATP peaks are not expected to have equal areas. The β peak is the smallest, the γ peak is larger, and the α peak is the largest. This can be clearly seen by simply visual inspection of Figs. 4b–4f. The phased absorption spectra obtained via the RELAX, FML, and SVD algorithms from the first 100 data samples without using any *a priori* knowledge about the peak locations are shown in Figs. 4b–4d, respectively. Note that seven of the eight peaks are properly identified by all the three methods and none of these methods can locate the peak of PME without using the *a priori* knowledge about the peak locations. Table 1 shows the approximate locations of the eight metabolite peaks estimated by three spectroscopy experts. The actual peak locations are assumed to be anywhere within the frequency intervals of length 0.23 ppm centered at the approximate locations given in Table 1. (We have assumed that only one dominant peak is located at each possible frequency interval.) With this *a priori* knowledge about the possible frequency intervals of the damped sinusoids, all eight metabolite peaks are identified by using E-RELAX and E-FML. It is found that the phased absorption spectra obtained via E-RELAX and E-FML fit well with the manually phased absorption spectrum obtained via 114° zero-order phasing, as can be seen clearly from Figs. 4e and 4f. (Note that a vertical offset is introduced in Figs. 4b–4f to show each spectrum clearly.)

Finally, consider 52 consecutively measured NMR spectroscopy datasets. Specifically, these data samples are 16-acquisition-averaged, phosphorus, NMR spectra obtained from the medial gastrocnemius muscle at 1.5 T (GE Signa) (TR = 2 s, unlocalized, 6-cm-diameter ^{31}P-tuned coil) while the volunteer rested (datasets 1–7), performed in-magnet exercise (datasets 8–28), and rested again (datasets 29–52). This type of dataset is difficult to analyze automatically due to the fast changing amplitudes, frequency locations (due to PH change), and peak overlap of the damped sinusoids. The *a priori* knowledge on the approximate frequency locations of the eight phosphorus metabolite peaks is determined and verified by three spectroscopy experts. Table 2 shows these approximate peak locations. The frequency interval of length 0.23 ppm is again used in this example. Figures 5a and 5b, respectively, show the eight metabolite peak estimates versus the dataset number using RELAX and FML. Since the NMR spectroscopy data are

TABLE 2
The Approximate Frequency Locations of the Eight ^{31}P Metabolite Peaks of the 52 Datasets Used in the Second Experimental Example

	Peak							
	STD	PME	P_i	PDE	PCr	γ-ATP	α-ATP	β-ATP
Frequency (ppm)	27.07	8.54	6.91	4.87	2.06	−0.13	−5.74	−14.08

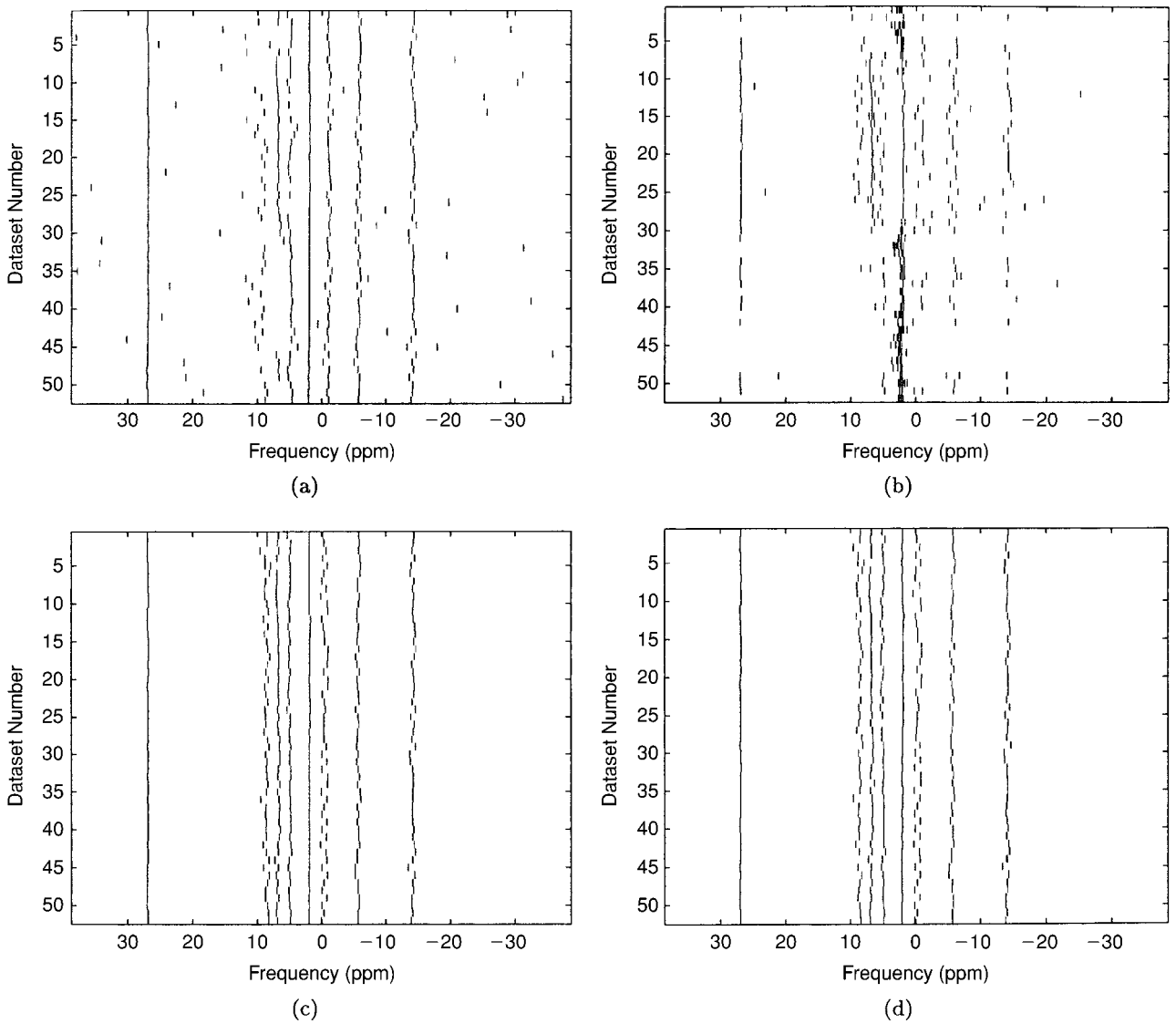

FIG. 5. Distribution of the eight ^{31}P metabolite peak estimates obtained via (a) RELAX, (b) FML, (c) E-RELAX, and (d) E-FML.

collected at a relatively low SNR and PME, P_i, and PDE are closely spaced and overlapped, RELAX and FML cannot provide consistent location (frequency) estimates of PME, P_i, and PDE for the 52-set measured data. In addition, both RELAX and FML will erroneously identify nose peaks as metabolite peaks. Note that frequency estimates via FML are worse than those via RELAX. More consistent frequency estimates can be obtained via E-RELAX and E-FML by using the *a priori* knowledge of the frequency intervals, as shown in Figs. 5c and 5d. In these figures there are no noise peaks identified as metabolites.

Figures 6 and 7, respectively, illustrate the relative areas corresponding to the parameter estimates of the eight ^{31}P metabolite peaks obtained via E-RELAX and E-FML. During exercise, it is expected that the amplitude of the STD peak will remain constant (within the limits of the signal-to-noise error), the P_i peak will increase, and the PCr peak will decrease. The other peak amplitudes are not expected to change during exercise. Following exercise, the P_i and PCr peak amplitudes are expected to return to their rest values. This is what is observed via E-RELAX and E-FML analyses, as illustrated by Figs. 6 and 7, respectively. However, E-FML analysis is more error-prone, as shown by the very low P_i peak amplitude for dataset 22 and very high P_i amplitudes for datasets 44 and 45. E-FML also shows large and spurious amplitude errors for the PME and PDE peaks, which can be seen from Figs. 7b and 7d. Analysis via E-RELAX more accurately reflects (within the limits of the

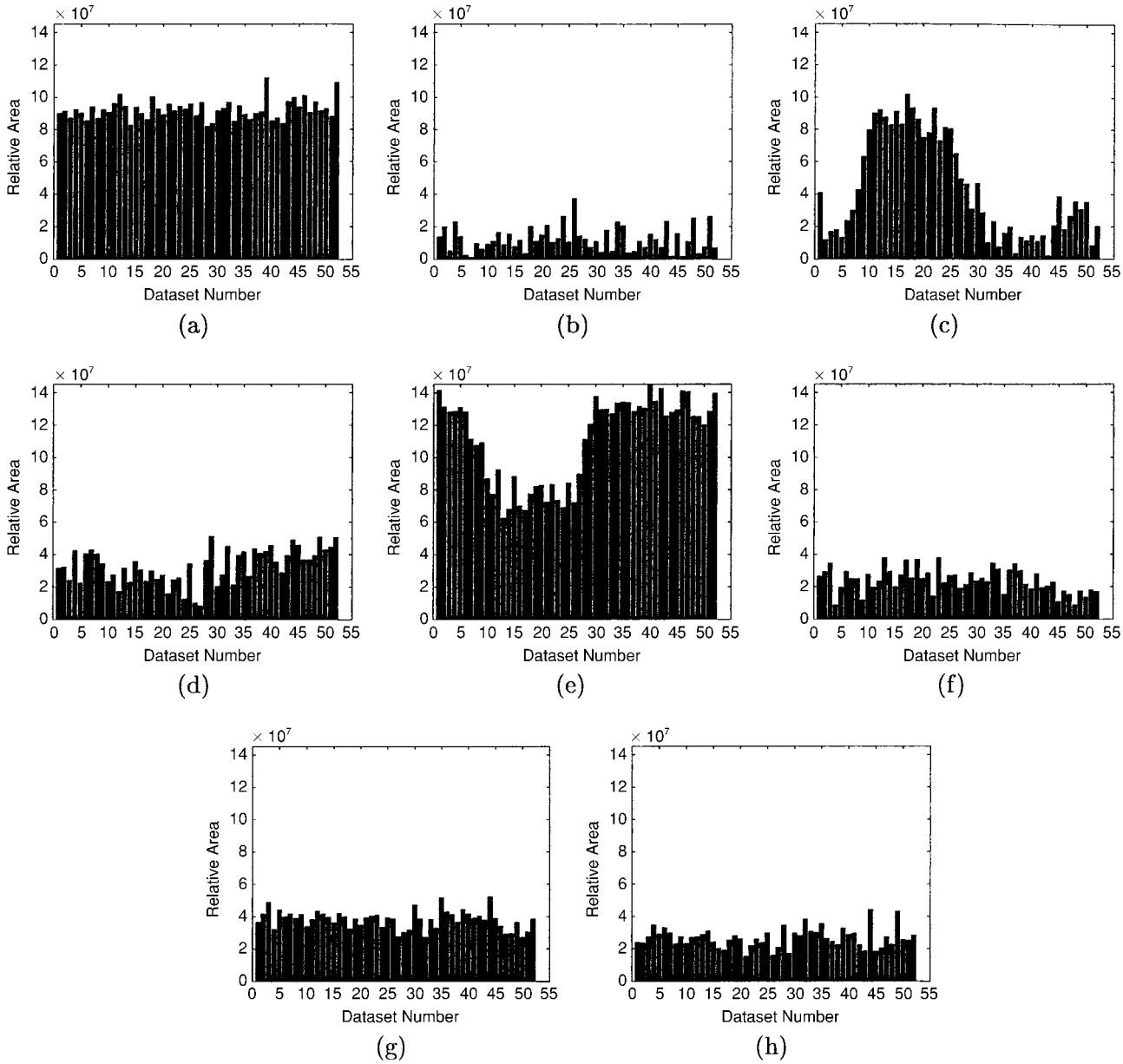

FIG. 6. Relative areas of the eight ^{31}P metabolite peaks versus the dataset number obtained via E-RELAX. (a) STD (an external standard of hexachlorocyclotriphosphazene (HCCTP) and chromium acetate (CrOAc) in benzene). (b) PME (phosphomonoester). (c) P_i (inorganic phosphate). (d) PDE (phosphodiester). (e) PCr (phosphocreatine). (f) γ-ATP. (g) α-ATP. (h) β-ATP.

signal-to-noise error) the expected metabolite level trends. For this example, the MATLAB flops required by RELAX, FML, E-RELAX, and E-FML are about 4.4×10^9, 5.1×10^9, 1.9×10^9, and 2.7×10^9, respectively.

4. CONCLUSIONS

In this paper, we have presented the E-RELAX algorithm and applied it to measured phosphorus (^{31}P) spectroscopy data. When the SNR of the recorded NMR spectroscopy data is low and there exist closely spaced damped sinusoids, the E-RELAX algorithm can still provide accurate parameter estimates due to using the *a priori* knowledge of the possible frequency intervals of the damped sinusoids, which is more flexible than the *a priori* knowledge of the exactly known frequency locations and damping ratios used by other methods. The quantification of the NMR spectroscopy data, including the analysis of the phased absorption spectra and the calculation of the relative areas corresponding to the metabolite peaks of interest,

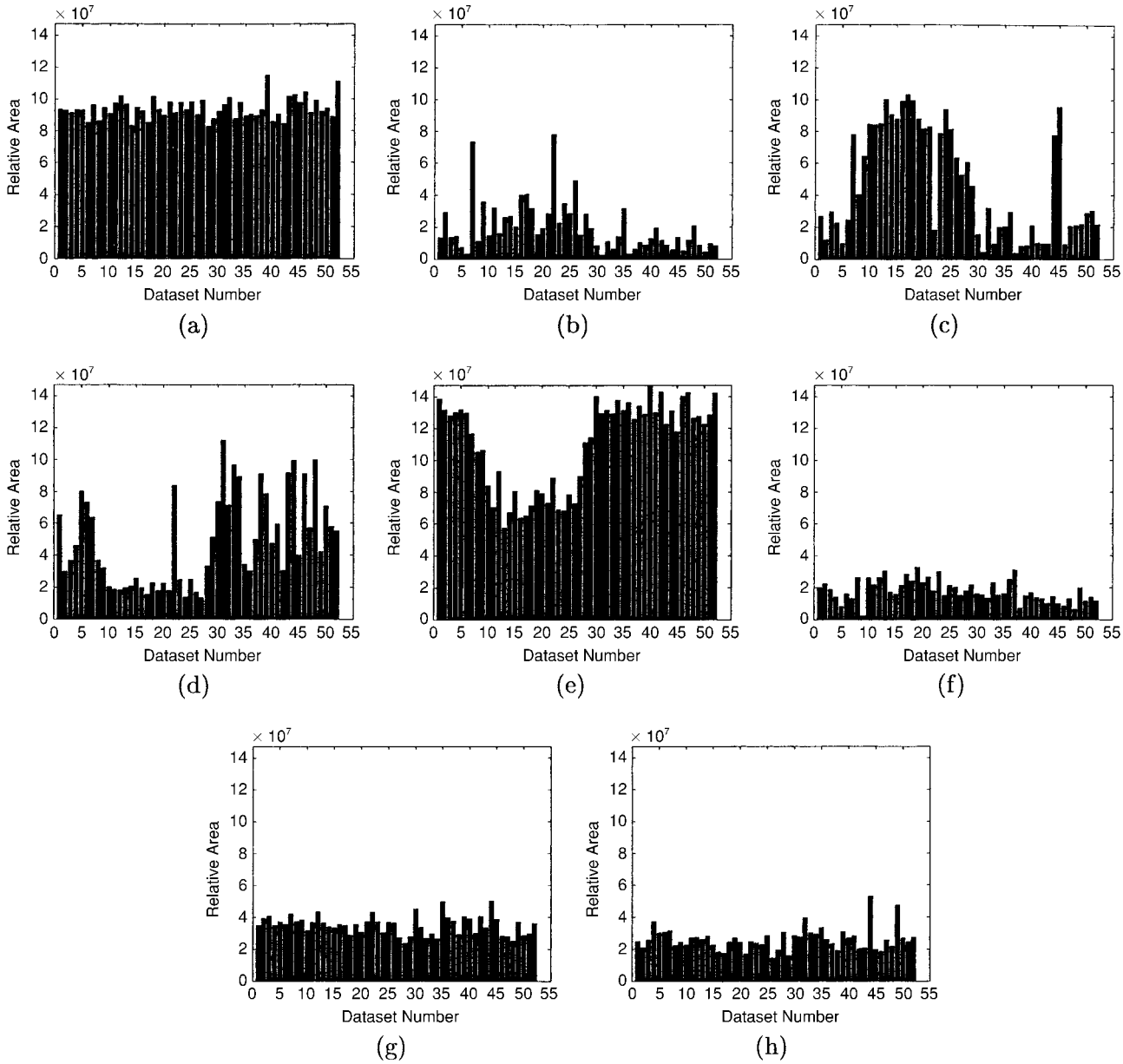

FIG. 7. Relative areas of the eight ^{31}P metabolite peaks versus the dataset number obtained via E-FML. (a) STD (an external standard of hexachlorocyclotriphosphazene (HCCTP) and chromium acetate (CrOAc) in benzene). (b) PME (phosphomonoester). (c) P_i (inorganic phosphate). (d) PDE (phosphodiester). (e) PCr (phosphocreatine). (f) γ-ATP. (g) α-ATP. (h) β-ATP.

can be accomplished readily by using the parameter estimates from E-RELAX.

REFERENCES

1. J. C. Hoch and A. S. Stern, "NMR Data Processing," Wiley, New York (1996).
2. V. Viti, P. Barone, L. Guidoni, and E. Massaro, Maximum entropy spectral analysis of ^{31}P NMR signals from human cells, *J. Magn. Reson.* **67,** 91–102 (1986).
3. V. Viti, E. Massaro, L. Guidoni, and P. Barone, The use of the maximum entropy method in NMR spectroscopy, *J. Magn. Reson.* **70,** 379–393 (1986).
4. G. J. Daniell and P. J. Hore, Maximum entropy and NMR—A new approach, *J. Magn. Reson.* **84,** 515–536 (1989).
5. J. A. Jones and P. J. Hore, The maximum entropy and Fourier transform method compared, *J. Magn. Reson.* **92,** 276–292 (1991).
6. J. Tang, C. P. Lin, M. K. Bowman, and J. R. Norris, An alternative to Fourier transform spectral analysis with improved resolution, *J. Magn. Reson.* **62,** 167–171 (1985).

7. D. W. Tufts and R. Kumaresan, Singular value decomposition and improved frequency estimation using linear prediction, *IEEE Trans. Acoust. Speech Signal Process.* **ASSP-30,** 671–675 (1982).
8. D. W. Tufts, R. Kumaresan, and I. Kirsteins, Data adaptive signal estimation by singular value decomposition of a data matrix, *Proc. IEEE* **70,** 684–685 (1982).
9. J. A. Cadzow, Signal enhancement—A composite property mapping algorithm, *IEEE Trans. Acoust. Speech Signal Process.* **36,** 49–62 (1988).
10. S. V. Huffel, Enhanced resolution based on minimum variance estimation and exponential data modeling, *Signal Process.* **33,** 333–355 (1993).
11. G. H. Golub and C. F. V. Loan, An analysis of the total least squares problem, *SIAM J. Numer. Anal.* **17,** 883–893 (1980).
12. H. Barkhuijsen, R. De Beer, and D. Van Ormondt, Improved algorithm for noninterative time-domain model fitting to exponentially damped magnetic resonance signals, *J. Magn. Reson.* **73,** 553–557 (1987).
13. R. A. Chylla and J. L. Markley, Theory and application of the maximum likelihood principle to NMR parameter estimation of multidimensional NMR data, *J. Biomol. NMR* **242**(5), 245–258 (1995).
14. S. Umesh and D. W. Tufts, Estimation of parameters of exponentially damped sinusoids using fast maximum likelihood estimation with application to NMR spectroscopy data, *IEEE Trans. Signal Process.* **44,** 2245–2259 (1996).
15. M. I. Miller and A. S. Greene, Maximum-likelihood estimation for nuclear magnetic resonance spectroscopy, *J. Magn. Reson.* **83,** 525–548 (1989).
16. Z.-S. Liu, J. Li, and P. Stoica, RELAX-based estimation of damped sinusoidal signal parameters, *Signal Process.* **62**(3) (1997).
17. E. M. Dowling, R. D. DeGroadt, and D. A. Linebarger, Exponential parameter estimation in the presence of known components and noise, *IEEE Trans. Antennas Propagation* **42,** 590–599 (1994).
18. H. Chen, S. Van Huffel, D. Van Ormondt, and R. De Beer, Parameter estimation with prior knowledge of known signal poles for the quantification of NMR spectroscopy data in the time domain, *J. Magn. Reson.* **119,** 225–234 (1996).
19. J. Van Der Veen, R. De Beer, P. R. Luyten, and D. Van Ormondt, Accurate quantification of *in vivo* ^{31}P NMR signals using the variable projection method and prior knowledge, *Magn. Reson. Med.* **6,** 92–98 (1988).
20. G. H. Golub and C. F. Van Loan, "Matrix Computations," Johns Hopkins Univ. Press, Baltimore, MD (1984).
21. J. Li and P. Stoica, Efficient mixed-spectrum estimation with applications to target feature extraction, *IEEE Trans. Signal Process.* **44,** 281–295 (1996).
22. P. Stoica, A. Jakobsson, and J. Li, Cisoid parameter estimation in the colored noise case: Asymptotic Cramér–Rao bound, maximum likelihood and nonlinear least-squares, *IEEE Trans. Signal Process.* **45,** 2048–2059 (1997).
23. W. I. Zangwill, "Nonlinear Programming: A Unified Approach," Prentice–Hall, Englewood Cliffs, NJ (1967).
24. V. G. Karmanov, "Programmation Mathematique," Editions Mir, Moscow (1977).
25. Z. Starcuk, Z. Starcuk, Jr., and J. Halámek, Correction of baseline and lineshape distortions in Fourier transform NMR spectroscopy by estimation of missing signals, *J. Magn. Reson.* **86,** 30–38 (1990).
26. E. C. Craig and A. G. Marshall, Automated phase correction of FT NMR spectra by means of phase measurement based on disperion versus absorption versus absorption relation (DISPA), *J. Magn. Reson.* **76,** 458–475 (1988).
27. A. V. Oppenheim and R. W. Schafer, "Discrete-Time Signal Processing," Prentice–Hall, Englewood Cliffs, NJ (1989).
28. P.-M. L. Robitaille, P. A. Robitaille, G. G. Brown, Jr., and G. G. Brown, An analysis of PH-dependent chemical-shift behavior of phosphorus-containing metabolites, *J. Magn. Reson.* **92,** 73–84 (1991).
29. P. R. Luyten, G. Bruntink, F. M. Soloff, J. W. A. H. Vermeulen, J. I. Van Der Heijden, J. A. Hollander, and A. Heershap, Broadband proton decoupling in human ^{31}P NMR spectroscopy, *NMR Biomed.* **1,** 177–183 (1989).
30. M. Rudin and A. Sauter, In vivo phosphorus-31 NMR: Potential and limitations, *NMR: Basic Princ. Prog.* **28,** 163–188 (1992).